Papain Entrapment in Alginate Beads for Stability Improvement and Site-Specific Delivery: Physicochemical Characterization and Factorial Optimization Using Neural Network Modeling

Mayur G. Sankalia,[1] Rajshree C. Mashru,[1] Jolly M. Sankalia,[1] and Vijay B. Sutariya[1]

[1]Center of Relevance and Excellence in NDDS, Pharmacy Department, The M.S. University of Baroda, Vadodara, Gujarat, India 390 002

ABSTRACT

This work examines the influence of various process parameters (like sodium alginate concentration, calcium chloride concentration, and hardening time) on papain entrapped in ionotropically cross-linked alginate beads for stability improvement and site-specific delivery to the small intestine using neural network modeling. A 3^3 full-factorial design and feed-forward neural network with multilayer perceptron was used to investigate the effect of process variables on percentage of entrapment, time required for 50% and 90% of the enzyme release, particle size, and angle of repose. Topographical characterization was conducted by scanning electron microscopy, and entrapment was confirmed by Fourier transform infrared spectroscopy and differential scanning calorimetry. Times required for 50% (T_{50}) and 90% (T_{90}) of enzyme release were increased in all 3 of the process variables. Percentage entrapment and particle size were found to be directly proportional to sodium alginate concentration and inversely proportional to calcium chloride concentration and hardening time, whereas angle of repose and degree of cross-linking showed exactly opposite proportionality. Beads with >90% entrapment and T_{50} of <10 minutes could be obtained at the low levels of all 3 of the process variables. The inability of beads to dissolve in acidic environment, with complete dissolution in buffer of pH ≥ 6.8, showed the suitability of beads to release papain into the small intestine. The shelf-life of the capsules prepared using the papain-loaded alginate beads was found to be 3.60 years compared with 1.01 years of the marketed formulation. It can be inferred from the above results that the proposed methodology can be used to prepare papain-loaded alginate beads for stability improvement and site-specific delivery.

Corresponding Author: Rajshree C. Mashru, Pharmacy Department, G.H. Patel Building, Donor's Plaza, The Maharaja Sayajirao University of Baroda, Fatehgunj, Vadodara, Gujarat, India 390 002. Tel: +91-265-2434187/2794051; Fax: +91-265-2418927; E-mail: sankalia_mayur@hotmail.com

INTRODUCTION

Papain (EC 3.4.22.2) is one of the thiol proteases, and its active site consists of Cys-25, His-159, and Asp-158. Papain shows extensive proteolytic activity toward proteins, short-chain peptides, amino acid esters, and amide links and is applied extensively in the fields of food and medicine. The reverse reaction of "papain hydrolysis," can be used in the synthesis of peptides and oligomers. Most marketed formulations containing papain and other digestive enzymes need to be stored at cold (2 to 8°C) or cool (8 to 25°C) temperatures conditions and still have the shelf-life of <1 year. Entrapment of the papain in ionotropically cross-linked biodegradable hydrogels may improve the stability of the parent enzymes and make it less prone to interference of various formulation excipients. Immobilized enzymes are stable at higher temperatures and might be stored at room temperature with extended shelf-life.[1] The optimum pH for activity of papain is in the range of 3 to 9, which varies with different substrates.[2] However, papain is almost inactive at a gastric pH of 1.2, so the ideal place for papain delivery is the small intestine. Multiple-unit dosage forms are particularly useful for the following purposes: (1) for delivering highly irritant drugs, such as nonsteroidal antiinflammatory drugs;[3] (2) for site-specific targeting of acid-labile drugs within the gastrointestinal tract;[4] and (3) for the delivery of enzymes, peptides/proteins, and vaccines.[5] The above advantages are of great commercial interest for the pharmaceutical industries; hence, it was the objective of the research to develop an extended shelf-life formulation for site-specific delivery of papain by immobilization in ionotropically cross-linked biodegradable alginate beads, which results in better and efficient utilization of enzymes. This article also deals with "in vitro" dissolution studies of beads, physicochemical characterization for evaluating the bead formation, and its release behavior.

Alginate, a high-molecular-mass polysaccharide, is a naturally occurring biodegradable copolymer of 1,4-linked β-D-mannuronic acid (M) and α-L-guluronic acid (G) that is extracted from brown seaweeds (*Phaeophyceae*, mainly *Laminaria*). It has been shown that the G and M units are joined together in blocks, and, as such, the following 3 types of blocks may be found: homo-polymeric G blocks

(GG), homopolymeric M blocks (MM), and heteropolymeric sequentially alternating blocks (MG). The reactivity with calcium and the subsequent gel formation capacity is a direct function of the average chain length of the G blocks. Hence, alginates containing the highest GG fractions possess the strongest ability to form gels. This initially arises from the ability of the divalent calcium cation to fit into the guluronate structures like eggs in an "egg box junction." Consequently, this binds the alginate chains together by forming junction zones, sequentially leading to gelling of the solution mixture and bead formation. When an aqueous solution of sodium alginate is added dropwise to an aqueous solution of calcium chloride, it forms a spherical gel with regular shape and size, also known as an "alginate bead." Alginate beads have the advantages of being nontoxic orally and having high biocompatibility.[6] Another advantageous property is their inability to reswell in acidic environment, whereas they easily reswell in an alkaline environment, so acid-sensitive drugs incorporated into the beads would be protected from gastric juice.[7] Therefore, alginate is used as an entrapment matrix for cells and enzymes, as well as for pharmaceutical and food adjuvants. In the past, conventional cross-linked calcium-alginate beads have been investigated for the development of a multiple-unit drug-delivery system.[8-11] However, not even a single reference could be cited in the literature to date for entrapment of papain in alginate beads for improvisation of shelf-life.

Neural network (NN) models might generalize better than regression models, because regression analyses are dependent on predetermined statistical significance levels (ie, less significant terms are not included in the model).[12,13] With the NN method, all of the data are used, potentially making the models more accurate. Hence, NN was selected as a modeling and evaluating tool in this article. The use of at least 1 hidden layer enables the NNs to describe nonlinear systems.[12] One layer is usually sufficient to provide an adequate prediction, even if continuous variables are adopted as the units in the output layer. Additionally, there is a little evidence to suggest that a larger number of hidden layers improves performance.[14]

The multilayer perceptron (MLP) with back propagation algorithm is one of the most widely implemented NN topologies and is important in the study of nonlinear dynamics. Two important characteristics of the MLP are its smooth nonlinear neurons (sigmoidal function) and its massive interconnectivity.

NN has been successfully applied to many pharmaceutical areas in recent years,[15] such as quantitative structure activity relationship analysis and drug modeling,[16] pharmacokinetic[17]-pharmacodynamic studies,[18] optimization and pharmaceutical formulation development,[14] powder flow,[19] compound determination using high-performance liquid chromatography,[20] analysis of nuclear magnetic resonance spectra,[21] prediction of drug release profile,[22] prediction of physicochemical properties,[23] prediction of octanol-water partition coefficient,[24] prediction of solubility,[25] and so forth.

MATERIALS AND METHODS

Materials

Hammersten-type casein US Pharmacopeia ([USP] Himedia Laboratories Pvt Ltd, Mumbai, India) and trichloroacetic acid (98.0%, Qualigens Fine Chemicals, Mumbai, India) were used as received. Purified papain Indian Pharmacopeia (IP), sodium alginate IP, calcium chloride dihydrate (98.0%), dibasic sodium phosphate (99.5%), disodium ethylenediaminetetraacetate (99.5%), cystein hydrochloride (99.0%), and citric acid (98.0%) were purchased from S. D. Fine-Chem Ltd (Mumbai, India). All of the other chemicals and solvents were of analytical grade and were used without additional purification. Deionized double-distilled water was used throughout the study.

Preparation of Beads

Concentrated sodium alginate solution in distilled water was prepared well before required. The required quantity of the enzyme (200 mg of papain in 50 mL of final sodium alginate solution) was dissolved in a small quantity of water and mixed with concentrated sodium alginate solution. The final concentration of sodium alginate was adjusted in the range of 1% to 2% w/v and was used after being degassed under a vacuum. The beads were prepared by dropping the sodium alginate solution (10 mL) containing papain from the dropping device, such as a syringe with a 26-gauge $\times$ 0.5-in flat-tip hypodermic needle, to a magnetically stirred calcium chloride solution (40 mL) at a rate of 5 mL/min and were allowed to harden for specific time. Different levels (Table 1) of sodium alginate, calcium chloride, and hardening time were selected. The beads were collected by decanting the calcium chloride solution, washed with deionized water, and dried to a constant weight in vacuum desiccator (Tarsons Products Pvt Ltd, Kolkata, India) at room temperature for 36 hours.

Factorial Design

In this study, a 3^3 full-factorial design was used to determine the effect of the sodium alginate concentration, the calcium chloride concentration, and the hardening time. Before the application of the design, a number of preliminary trials were conducted to determine the conditions at which the process resulted to beads. The matrix of the experiments and the results of the responses are listed in

Table 1. Process Variables and Their Levels for 3^3 Full-Factorial Design

Factors	Low Level	Middle Level	High Level
Sodium alginate (% w/v)	1.0	1.5	2.0
Calcium chloride (M)	0.05	0.10	0.15
Hardening time (min)	20	25	30

Table 2. To determine the experimental error, the experiment at the center point was repeated 5 times at different days. The mean (±SD) percentage of entrapment, time required for 50 (T_{50}) and 90 (T_{90}) percent of enzyme release, particle size, and angle of repose of these experi-

ments were 85.88 ± 1.02%, 15.57 ± 0.28 min, 82.43 ± 0.33 min, 261.1 ± 0.9 μm, and 20.61 ± 0.29°, respectively. The above-mentioned values showed good reproducibility of the process.

NN Software and Network Topology

The Microsoft Windows-based NN software NeuroSolutions Version 4.24 (NeuroDimension, Inc) was used. The MLP with single hidden-layer architecture was chosen. The experimental matrix of 32 input-to-desired output data sets (Table 2) was introduced in to the model, with 3 input neurons (process variables), 1 hidden layer, and 5 output neurons (response variables). Various adjustable parame-

Table 2. Matrix of the Experiments and Results for the Measured Responses

	Factors/ Levels			Responses				
ES*	Na Alginate (% w/v)	Calcium chloride (M)	Hardening Time (min)	% Entrapment	T_{50}	T_{90}	Size (μm)	Angle of Repose
1	1.0	0.05	20	91.80	6.50	23.80	211.1	22.62
10	1.0	0.05	25	89.00	8.30	25.70	207.3	22.88
19	1.0	0.05	30	86.20	9.35	28.40	202.6	23.27
4	1.0	0.10	20	85.00	7.80	27.50	184.3	23.39
13	1.0	0.10	25	82.60	9.10	30.55	181.1	23.75
22	1.0	0.10	30	80.71	10.70	34.00	178.3	24.15
7	1.0	0.15	20	68.80	8.60	34.60	176.0	24.07
16	1.0	0.15	25	67.79	10.30	39.00	171.4	24.94
25	1.0	0.15	30	65.28	12.05	59.25	169.7	26.33
2	1.5	0.05	20	93.40	13.35	48.00	297.0	19.50
11	1.5	0.05	25	90.80	14.45	57.40	291.6	19.76
20	1.5	0.05	30	88.00	16.30	57.40	285.5	20.02
5	1.5	0.10	20	87.70	14.35	75.00	266.9	20.27
29	1.5	0.10	25	87.01	15.30	82.50	261.5	20.56
32	1.5	0.10	25	86.29	15.90	82.90	259.8	20.20
31	1.5	0.10	25	85.06	15.20	82.40	260.3	20.98
28	1.5	0.10	25	84.35	15.80	81.90	261.9	20.44
14	1.5	0.10	25	86.78	15.70	82.30	262.0	20.89
30	1.5	0.10	25	85.80	15.50	82.60	261.3	20.58
23	1.5	0.10	30	83.50	16.80	87.65	255.4	20.97
8	1.5	0.15	20	77.30	15.55	80.55	258.2	21.20
17	1.5	0.15	25	75.30	16.90	83.50	252.7	21.84
26	1.5	0.15	30	72.00	19.30	86.50	246.0	22.20
3	2.0	0.05	20	94.40	15.90	83.80	715.3	16.14
12	2.0	0.05	25	91.39	17.05	91.50	708.0	16.49
21	2.0	0.05	30	88.50	18.60	95.60	701.3	16.87
6	2.0	0.10	20	88.40	17.70	90.80	682.7	17.00
15	2.0	0.10	25	86.00	18.60	94.20	677.1	17.26
24	2.0	0.10	30	84.00	20.20	96.15	671.9	17.77
9	2.0	0.15	20	79.50	19.40	95.60	673.5	18.03
18	2.0	0.15	25	76.60	20.40	96.30	668.2	18.56
27	2.0	0.15	30	73.70	22.80	97.20	662.7	18.89

*ES indicates experimental sequence.

ters, like the number of neurons in the hidden layer, the step size, the momentum of the hidden layer and the output layer, and so forth, were optimized. Training was repeated 3 times for optimization of all of the parameters. At the start of the training run, weights were initialized with random values. During training, 5 additional data sets of input-to-desired output ratio were used for the cross-validation and were back-propagated through the network to evaluate the trained network. The training termination criterion was the rise in minimum standard error of the cross-calibration set compared with that of the training set for 100 continuous epochs. The network trained under optimum conditions was used to predict the responses at different factor values and response surfaces were generated for interpretation.

Characterization of Beads

Estimation of Papain

Papain was estimated by modified casein digestion method of USP XXVI in the presence of cysteine hydrochloride. Different aliquots of standard papain solution in phosphate-cysteine disodium ethylenediaminetetraacetate buffer were added to 5 mL of buffered substrate (hammersten-type casein 10 mg/mL, pH 6.0 $\pm$ 0.1) and incubated for 60 minutes at 40°C. The digestion process of casein was stopped by adding 3 mL of 30% w/v trichloroacetic acid solution and was allowed to stand for 30 to 40 minutes at 40°C. Digested amino acids were filtered through Whatman filter paper no. 42 by discarding first 3 mL of filtrate, and absorbance was measured at 280 nm against their respective blanks. The method was found to be linear over an analytical range of 3 to 100 μg/mL with a correlation coefficient (r) of 0.9996. Limit of detection, limit of quantitation, and regression equation were found to be 0.77 μg/mL, 2.57 μg/mL, and y = 0.0042x $-$ 0.0033, respectively.

Determination of Entrapment Efficiency

Entrapment efficiency was determined by dissolving the enzyme-loaded beads in a magnetically stirred simulated intestinal fluid without enzyme (USP XXVI) for about 45 minutes. The resulting solution was centrifuged at 2,500 rpm for 10 minutes (Remi Instruments Ltd, Mumbai, India), and the supernatant was assayed (n = 3) for enzyme content by the modified casein digestion method of USP XXVI. Entrapment efficiency was calculated as:

$$\text{Entrapment efficiency} = \frac{\text{Enzyme loaded}}{\text{Theoratical enzyme loading}} \times 100 \qquad (1)$$

Effect of pH on Release Profile

To study the effect of pH on the papain release profile, an in vitro dissolution study was conducted using the USP XXVI dissolution apparatus 2 (TDT-60T, Electrolab, Mumbai, India) in 500 mL of different pH media (simulated gastric juice pH 1.2 [USP], phosphate buffer pH 4.0 [IP], neutralized phthalate buffer pH 5.4 [IP], simulated intestinal fluid without enzyme pH 6.8 [USP], phosphate buffer pH 7.4 [IP], and phosphate buffer pH 8.0 [IP]) on the optimized batch at 37 $\pm$ 0.5°C with a paddle speed of 75 rpm. Accurately weighed samples (n = 3) equivalent to about 40 mg of papain were introduced to dissolution media, and samples of 2 mL were collected at 0, 0.25, 0.50, 0.75, 1.0, 1.5, 2.0, 2.5, 3.0, 3.5, 4.0, 4.5, 5.0, 5.5, and 6.0 hours. Samples were filtered through a 0.4-μm Whatman membrane filter and assayed for enzyme content as before.

Determination of T_{50} and T_{90}

T_{50} and T_{90} are important parameters for the enzyme release study and were used to evaluate the onset of action and duration of action, respectively. For optimization purposes, a dissolution study of all of the batches was conducted in 500 mL of simulated intestinal fluid without enzyme as before. Accurately weighed samples (n = 3) equivalent to about 40 mg of papain were subjected to dissolution, and aliquots of 2 mL were assayed at 0, 5, 10, 15, 20, 30, 45, 60, 90, and 120 minutes. T_{50} and T_{90} were found by extrapolating the percentage of enzyme released versus time plot.

Particle Size Measurements

Particle size is an important parameter for the formulation development. An optimized batch of the beads was filled in the capsules during which the particle size was the evolutionary parameter. Larger particles show higher weight variation during capsule filling; hence, the experimental conditions resulting in smaller particles are preferable. Particle size was determined with the laser diffraction particle size analyzer (MAN 0244/HYDRO 2000 SM, Malvern Instruments Ltd, Malvern, United Kingdom) using isopropyl alcohol as a vehicle.

Angle of Repose Measurements

Angle of repose was measured for estimating flowability of the beads. If the angle exceeds 50°, the material will not flow satisfactorily, whereas materials having values near the minimum flow easily and well. The rougher and more irregular the surface of the particles, the higher the angle of repose. The angle also increases with decrease in particle size. The angle of repose was measured by passing beads through a funnel on the horizontal surface. The height (*h*)

of the heap formed was measured with a cathetometer, and the radius (*r*) of the cone base was also determined. The angle of repose (Φ) was calculated from:

$$\tan \Phi = \frac{h}{r} \qquad (2)$$

Fourier Transform Infrared Spectroscopy

Infrared transmission spectra were obtained using a Fourier transform infrared spectroscopy (FTIR) spectrophotometer (FTIR-8300, Shimadzu, Japan). A total of 5% (w/w) of sample, with respect to the potassium bromide (KBr) disk, was mixed with dry KBr (S. D. Fine Chem Ltd, Mumbai, India). The mixture was ground into a fine powder using an agate mortar before compressing into the KBr disk under a hydraulic press at 10,000 psi. Each KBr disk was scanned at 4 mm/s at a resolution of 2 cm over a wave number region of 400 to 4,500 cm^{-1}. The characteristic peaks were recorded.

Differential Scanning Calorimetry

Differential scanning calorimetric analysis was used to characterize the thermal behavior of the isolated substances, their physical mixture, and empty and loaded beads. Differential scanning calorimetry (DSC) thermograms were obtained using an automatic thermal analyzer system (DSC-60, Shimadzu, Japan). Temperature calibration was performed using indium as a standard. Samples were crimped in a standard aluminum pan and heated from 40 to 400°C at a heating rate of 10°C/min under constant purging of dry nitrogen at 30 mL/min. An empty pan, sealed in the same way as the sample, was used as a reference. The characteristic endothermic peaks and specific heat of the melting endotherm were recorded.

Scanning Electron Microscopy

The purpose of the scanning electron microscopy study was to obtain a topographical characterization of beads. The beads were mounted on brass stubs using double-sided adhesive tape. Scanning electron microscopy photographs were taken with a scanning electron microscope (JSM-5610LV, Jeol Ltd, Tokyo, Japan) at the required magnification at room temperature. The working distance of 39 mm was maintained, and the acceleration voltage used was 15 kV, with the secondary electron image as a detector.

Preparation of Capsule Formulation, Packaging, and Stability Study

Accurately weighed alginate beads equivalent to 40 mg of papain were filled into a hard gelatin capsule manually.

The joint of the capsule body and cap was carefully sealed by pressing them to fit in the lock mechanism. The capsules were packaged in high-density polyethylene bottles with polypropylene caps (foamed polyethylene and pressure sensitive liner). The capsules were subjected to stability testing according to the International Conference on Harmonization guidelines for zone III and IV. The packed containers of prepared capsules along with marketed formulation and bulk papain were kept for accelerated (40 ± 2°C/75 ± 5% relative humidity) and long-term (30 ± 2°C/65 ± 5% relative humidity) stability in desiccators with saturated salt solution for up to 12 months. A visual inspection (for discoloration of capsule content), dissolution testing, and papain content estimation was conducted every 15 days for the entire period of stability study.

RESULTS AND DISCUSSION

Optimization of NN

For the optimum number of neurons in the hidden layer, the NN was trained with 1 to 35 hidden neurons with 2,000 training epochs, and performance was tested after the addition of each neuron and was found to be 17. Step size, momentum of hidden, and output layer were optimized by varying the parameters from 0.1 to 1 at the increment of 0.1. The optimum step size for hidden layer and output layer was found to be 0.9 and 1, respectively, whereas the optimum momentum for hidden layer and output layer was found to be 0.9. The NN was constructed using the optimum conditions and was used to predict the experimental matrix (Table 3) and to generate the response surfaces for interpreting the effect of various process variables.

Effect of the Factors on Responses

Percentage of Entrapment

Contour plots of response surface for percentage of entrapment are shown in Figure 1A, C, and E, from which it can be concluded that the >90% of the entrapment value was obtained at the high level (2% w/v) of the sodium alginate concentration, especially when the high level of the sodium alginate concentration was followed by the low levels of the other 2 factors (94.4% entrapment, experiment 3; Table 2). Whereas the calcium chloride concentration and hardening time were affecting negatively (ie, response decreases with an increase in factor level) in a significant amount, their interaction was synergistic at higher levels (experiment 25, 26, and 27; Table 2).

On the addition of sodium alginate solution to a calcium chloride solution, instantaneous interfacial cross-linking takes place with precipitation of calcium alginate followed by a more gradual gelation of the interior, which causes loss of enzyme from the surface of the beads. This can be

Table 3. Matrix of the Experiments and NN-Predicted Responses

	Factors/ Levels			Responses				
Sr. No.	Na Alginate (% w/v)	Calcium Chloride (M)	Hardening Time (min)	% Entrapment	T_{50}	T_{90}	Size (µm)	Angle of Repose
1	1.0	0.05	20	91.81	7.45	22.09	151.0	22.45
2	1.0	0.05	25	89.93	8.31	23.26	150.3	22.92
3	1.0	0.05	30	87.28	9.44	24.94	149.4	23.43
4	1.0	0.10	20	84.23	8.00	26.94	151.0	23.37
5	1.0	0.10	25	81.61	9.28	31.09	150.0	23.89
6	1.0	0.10	30	78.63	10.87	36.27	148.8	24.43
7	1.0	0.15	20	69.87	8.46	34.30	150.5	24.31
8	1.0	0.15	25	68.70	10.14	43.54	149.2	24.84
9	1.0	0.15	30	67.78	12.21	54.11	147.7	25.33
10	1.5	0.05	20	93.04	12.29	51.25	300.2	19.10
11	1.5	0.05	25	91.31	13.77	57.76	292.1	19.50
12	1.5	0.05	30	88.69	15.11	62.82	283.9	19.94
13	1.5	0.10	20	88.81	13.96	72.34	275.5	20.18
14	1.5	0.10	25	86.17	15.89	80.51	269.5	20.65
15	1.5	0.10	30	82.90	17.49	85.84	262.6	21.17
16	1.5	0.15	20	76.07	14.94	81.70	257.0	21.32
17	1.5	0.15	25	74.14	17.20	89.34	250.9	21.86
18	1.5	0.15	30	72.35	18.94	93.72	242.5	22.48
19	2.0	0.05	20	92.80	16.31	84.32	699.8	16.67
20	2.0	0.05	25	91.04	17.59	88.50	698.5	16.82
21	2.0	0.05	30	88.54	18.64	91.26	696.6	16.99
22	2.0	0.10	20	89.04	17.89	92.74	684.8	17.18
23	2.0	0.10	25	86.16	19.16	95.39	682.1	17.40
24	2.0	0.10	30	82.77	20.13	97.03	678.6	17.67
25	2.0	0.15	20	79.81	19.23	96.34	661.9	17.93
26	2.0	0.15	25	76.91	20.38	98.09	657.4	18.25
27	2.0	0.15	30	74.28	21.20	99.10	651.5	18.63

noticed from the pores on the bead surface (Figure 2) created by the water-soluble macromolecules both because it affected the calcium alginate network formation during the unit preparation and because it was leached from the membrane into the medium.[26] Loss of surface enzyme was found to be proportional to the degree of cross-linking. Increase in viscosity with an increase in sodium alginate concentration retarded penetration of calcium to the interior of the bead, resulted in decreased cross-linking (also decreased surface roughness and porosity; Figure 2A–C), and increased entrapment efficiency. Degree of cross-linking increases with an increase in calcium concentration and contact time;[27] hence, entrapment efficiency decreased.

T_{50}

As shown in Figure 1A, C, and E, all 3 of the factors had significant positive (ie, response increases with increase in factor level) effects on the response value. However, immediate release of enzyme for quicker onset of action

and, hence, shorter T_{50} was the desirable criteria for the optimum formulation; hence, low value of all 3 of the variables resulted in the beads with T_{50} as low as 6.5 minutes (experiment 1, Table 2). T_{50} was found to be proportional to the particle size and degree of cross-linking. As the concentration and, hence, the viscosity of alginate solutions increases, larger beads (discussed under "Particle Size," below) with less surface porosity (Figure 2A–C) were obtained, which took a long time for complete dissolution and resulted in higher T_{50} (16 to 23 minutes; Table 2). Higher calcium concentration and hardening time caused penetration of calcium to the interior of the bead, resulted in increased cross-linking[27] (also increased surface roughness and porosity; Figure 2D–F), and delayed dissolution (hence, higher T_{50}).

T_{90}

As with T_{50}, all 3 of the factors had positive effects on this response, which can be observed in Figure 1B, D, and F.
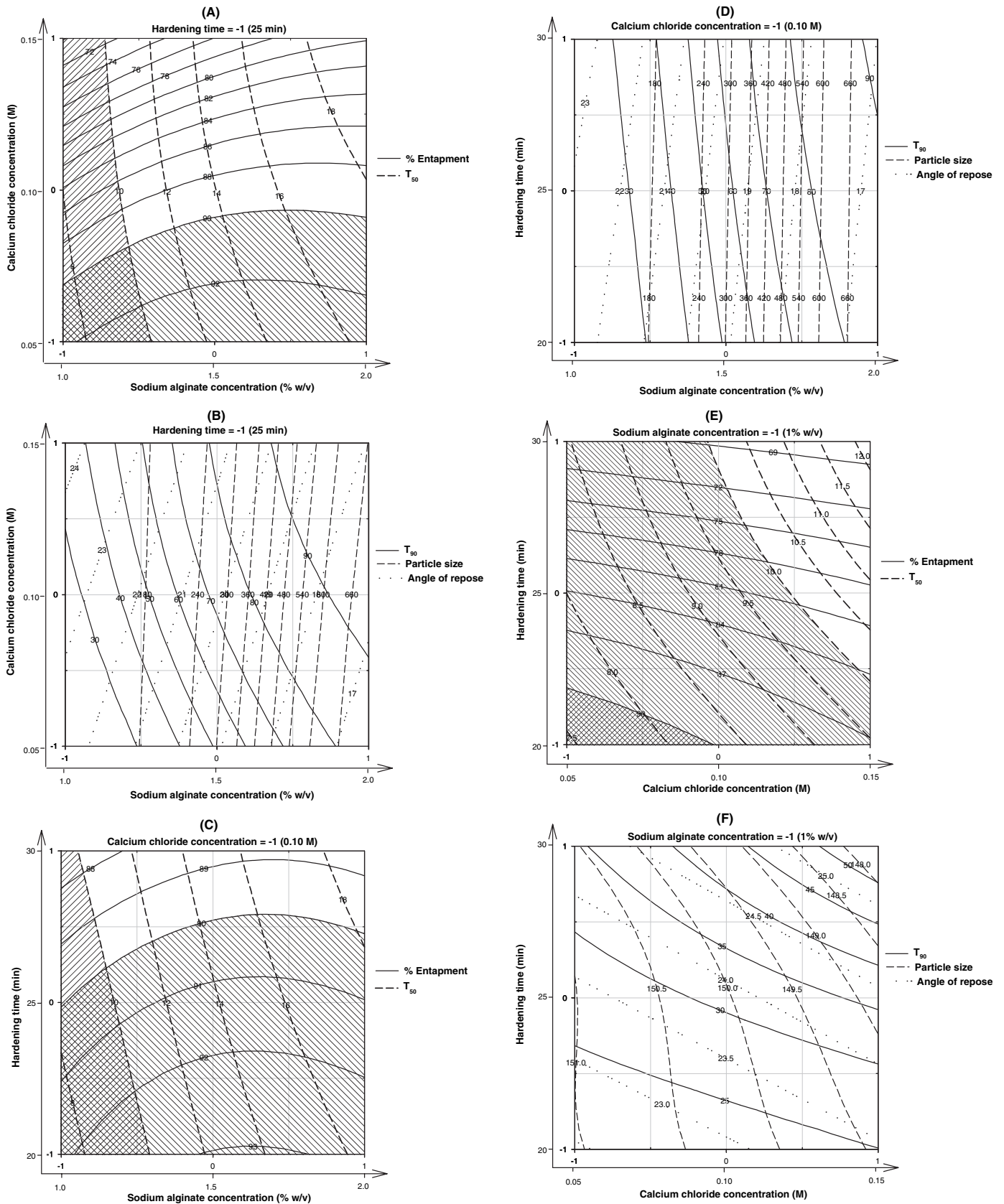
Figure 1. Contour plots of percentage of entrapment, T_{50}, T_{90}, particle size, and angle of repose as a function of sodium alginate concentration, calcium chloride concenstration, and hardening time.
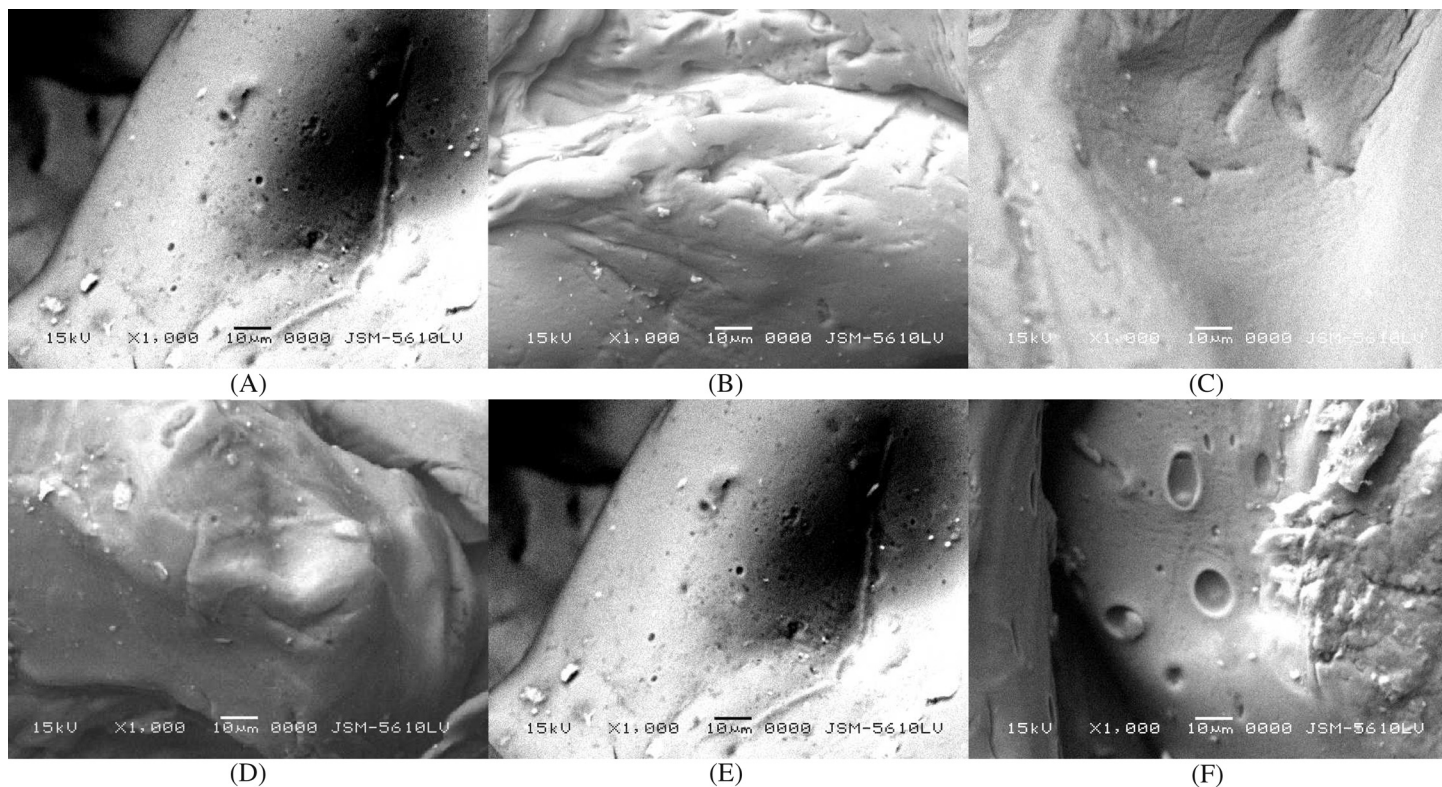
Figure 2. Scanning electron microscopy micrographs and surface morphology of calcium alginate beads. (A–C) Effect of sodium alginate concentration on surface morphology (calcium chloride concentration 0.15 mol/L): (A) 1.0% w/v, (B) 1.5% w/v, and (C) 2.0% w/v sodium alginate concentration. (D–F) Effect of calcium chloride concentration on surface morphology (sodium alginate concentration 1.5% w/v): (D) 0.10 mol/L, (E) 0.15 mol/L, and (F) 0.20 mol/L calcium chloride concentration.

The sodium alginate concentration was the most positively influencing factor among all 3 (higher T_{90} of the magnitude of 83 to 98 minutes; Table 2). None of the remaining 2 factors was affecting T_{90} significantly. However, both calcium chloride concentration and hardening time at higher levels had a synergistic positive action (experiment 25, 26, and 27; Table 2). T_{90} was also found to be proportional to the particle size and degree of cross-linking. For additional explanation, see "T_{50}" section, above.

Particle Size

As shown in Figure 1B, D, and F, the sodium alginate concentration was the most affecting factor. The bead size is influenced by the opening through which the alginate solution is allowed to pass (which was kept constant) and the viscosity of the alginate solution. Increased viscosity at a higher concentration of sodium alginate resulted in larger particles (660 to 715 μm; Table 2). Calcium chloride concentration and hardening time had a negative effect on the particle size. High calcium chloride concentration and hardening time caused shrinkage of beads and resulted in smaller particle size (experiment 25, 26, and 27; Table 2) because of a high degree of cross-linking.[27] Although the negative effect of calcium chloride concentration and hard-

ening time was of less magnitude, they contribute to the morphology of the beads, and the surface became rougher and porous (Figure 2D–F).

Angle of Repose

Here, too, the sodium alginate concentration had a significant positive effect on the angle of repose. However, calcium chloride concentration and hardening time had a synergistic positive effect at higher levels (experiment 25, 26, and 27; Table 2); their individual effects were negligible. Particle size increased with the increase in sodium alginate concentration and resulted in a decreased angle (lowest angle of 16.14, experiment 3; Table 2). Higher calcium chloride concentration and hardening time resulted in smaller beads with irregular surface because of shrinkage and showed an increased angle (from 16.14 to 18.89 in experiments 3 to 27, respectively).

Optimization of the Process Using the Graphical Evaluation

Generally, the aim of the optimization of pharmaceutical formulations is to find the optimum levels of the variables, which affect a process, where a product of good character-

Table 4. Comparison of Responses Between Predicted and Experimental Values for the Cross-Validation Set

Responses	Test	Factors/Levels			Experimental Values	Predicted Values	Bias %
		A	B	C			
% Entrapment	1	−1	−0.6	−0.6	90.72	89.04	1.9
	2	−0.6	0	0.4	81.15	82.98	2.2
	3	−0.4	0.6	0	76.01	77.65	2.1
	4	0	−0.4	0.6	84.58	87.13	2.9
	5	0.4	0.4	−0.4	86.06	84.17	2.2
T_{50}	1	−1	−0.6	−0.6	7.81	8.04	2.9
	2	−0.6	0	0.4	12.83	12.79	0.4
	3	−0.4	0.6	0	14.47	14.31	1.1
	4	0	−0.4	0.6	16.23	16.07	1.0
	5	0.4	0.4	−0.4	17.09	17.58	2.7
T_{90}	1	−1	−0.6	−0.6	24.68	24.27	1.7
	2	−0.6	0	0.4	56.33	54.47	3.4
	3	−0.4	0.6	0	72.15	73.18	1.4
	4	0	−0.4	0.6	75.61	76.88	1.7
	5	0.4	0.4	−0.4	88.63	90.90	2.5
Particle Size	1	−1	−0.6	−0.6	161.7	150.7	7.3
	2	−0.6	0	0.4	180.7	166.2	8.8
	3	−0.4	0.6	0	172.8	182.6	5.4
	4	0	−0.4	0.6	285.9	273.8	4.4
	5	0.4	0.4	−0.4	414.6	435.0	4.7
Angle of Repose	1	−1	−0.6	−0.6	22.29	23.01	3.1
	2	−0.6	0	0.4	21.95	22.98	4.5
	3	−0.4	0.6	0	23.56	22.78	3.4
	4	0	−0.4	0.6	19.89	20.47	2.8
	5	0.4	0.4	−0.4	18.90	19.44	2.8

istics could be produced. NN can be trained for predicting the response surface and can be used for optimization within the experimental region. Contour plot of the NN-predicted responses affected by 2 chosen variables are shown in Figure 1A–F. The contours represent different combinations of 2 variables with the same response. Two responses, namely the percentage of entrapment and T_{50}, were selected for optimization of the process. The criteria for the optimum formulation selection were >90% entrapment and T_{50} of <10 minutes. From observing these figures, it is clear that the >90% entrapment area coincides with the T_{50} area of <10 minutes. The study of these plots showed that the highest values of the entrapment and lowest value of T_{50} could be obtained at low values of all 3 of the process variables (ie, at −1, −1, and −1; experiment 1, Table 2).

Evaluation of Model Using Cross-Validation

To assess the reliability of the model, 5 cross-validation experiments were conducted by varying the process variables at values other than that of the model, and responses were predicted using the trained network. A comparison between the experimental and predicted values of the responses for these additional experiments is presented in Table 4. Bias was calculated by the following equation:

$$\text{Bias} = \left[\frac{(\text{predicted value} - \text{experimental value})}{\text{predicted value}}\right] \times 100$$

(3)

It can be seen that in all of the cases there was a reasonable agreement between the NN predicted and the experimental value, because a low value of the bias was found. For this reason, it can be concluded that the NN-predicted responses describe adequately the influence of the selected process variables on the responses under study, and NN can be used successfully as a predictive and optimizing tool.

Characterization of Optimal Formulation

Effect of pH on Release Profile

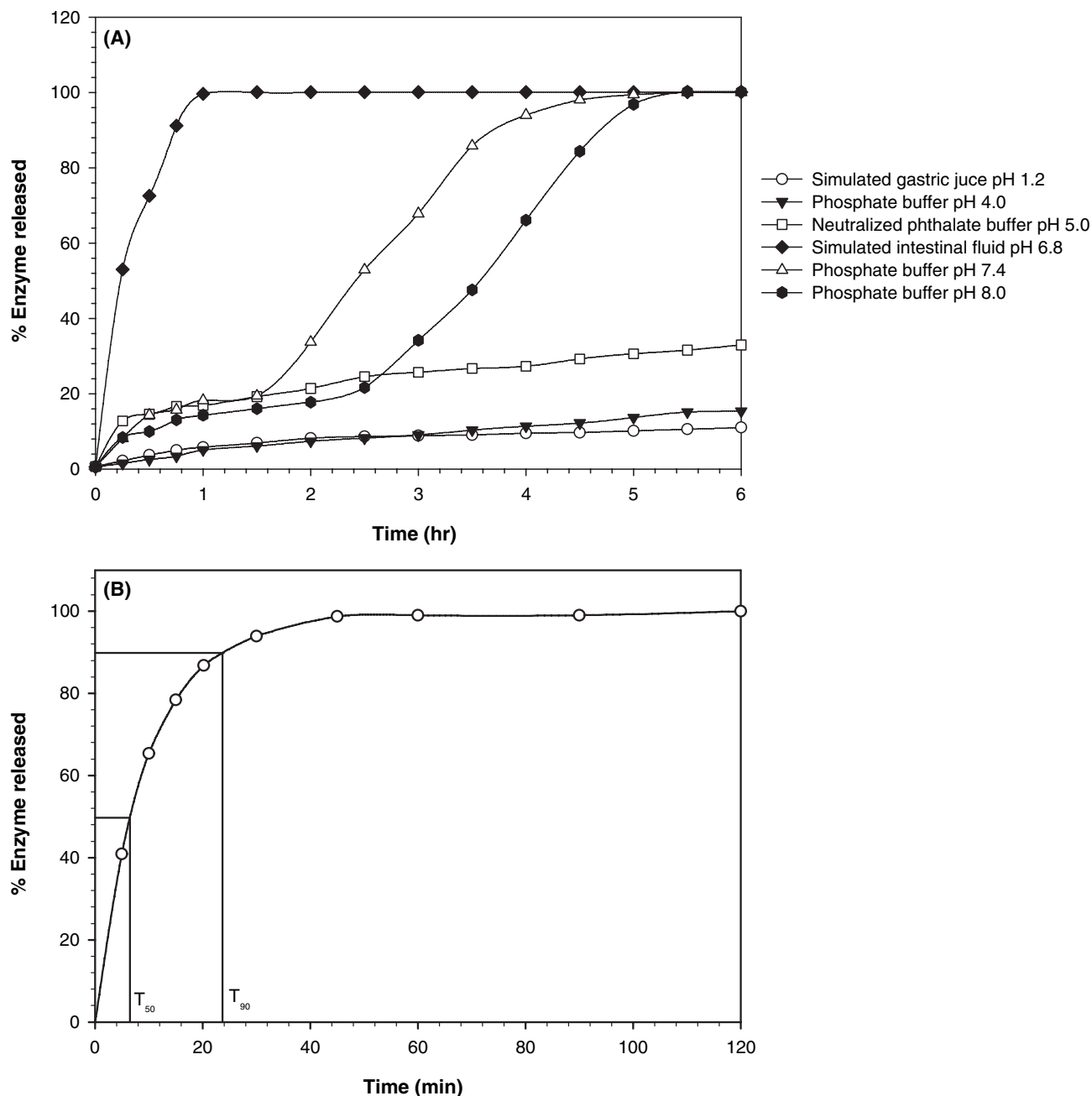The effect of pH on the release of papain from calcium alginate beads in different pH (1.2, 4.0, 5.4, 6.8, 7.4, and

Figure 3. (A) The effect of pH on the release profile of papain in different buffers simulating the human gastrointestinal tract; (B) In vitro release profile of optimized batch in simulated intestinal fluid without enzyme.

8.0) buffers simulating the human gastrointestinal tract is given in Figure 3A. Release profile of optimized batch in simulated intestinal fluid without enzyme is shown in Figure 3B. Generally, higher molecular weight and poorly water-soluble drugs are not released from calcium alginate beads because of stability and nonswelling property in the acidic environment, whereas swell and disintegrate is found in intestinal fluid.[7,28] This was additionally confirmed by the very low amount of papain release in the acidic media (pH 1.2, 4.0, and 5.4) because of higher molecular weight. The swelling and disintegration of calcium alginate beads are dependent on compositions of dissolution medium, for example, sodium and phosphate,

and solubility of drug entrapped into alginate beads.[29] The swelling and disintegration of alginate beads in intestinal fluid (pH 6.8) were attributable to the affinity of calcium to phosphate and sodium/calcium exchange. However, the complete release profile was delayed up to 6 hours as the pH increased (7.4 and 8.0) despite the presence of sodium and phosphate. This study confirms the site-specific papain delivery to the intestine rather than the stomach.

FTIR

FTIR spectra of papain, sodium alginate, calcium alginate blank beads, papain-loaded optimized batch, and the
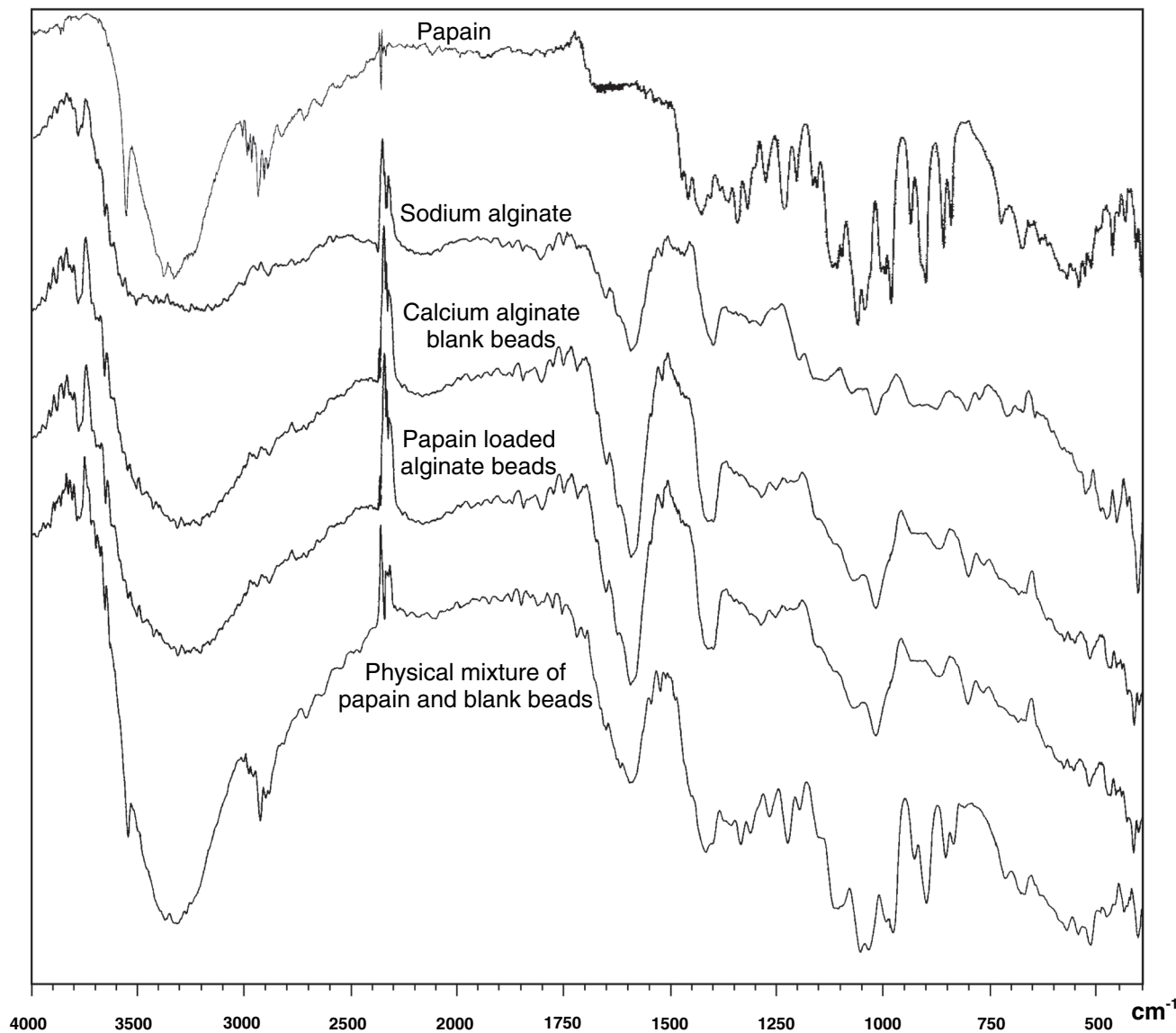
Figure 4. The FTIR spectra of papain, sodium alginate, blank calcium alginate beads, papain-loaded alginate beads, and physical mixture of papain and blank calcium alginate beads.

physical mixture of papain and blank beads are shown in Figure 4. FTIR spectrum of sodium alginate powder showed various distinct peaks of alginate: hydroxyl at 3,263.33 cm^{-1}, carbonyl at 1,600.81 cm^{-1}, and carboxyl and carboxylate at about 1,000 to 1,400 cm^{-1} (Figure 4). Cross-linking of alginate by Ca^{2+} was shown by a decrease in the wave number of the carbonyl peak from 1,600.81 to 1,579.32 cm^{-1}. The hydroxyl peak of calcium alginate had a higher value of wave number than that of the sodium alginate (Figure 4). This was probably because of a negative effect on bond formation involving adjacent hydroxyl groups as a result of conformational changes of alginate after reacting with Ca^{2+}.[30] With incorporation of papain, the spectrum of beads (Figure 4) was similar to that of the calcium alginate blank beads (Figure 4). However, the physical mixture of papain and calcium alginate blank beads showed the peaks attributable to both papain and calcium alginate. This confirms the papain entrapment into the alginate beads at the molecular level.

DSC

The DSC thermograms of papain, sodium alginate, blank calcium alginate beads, and papain-loaded beads are shown in Figure 5. The degradation exotherm of sodium alginate at 252°C was absent in blank calcium alginate bead, and an additional endothermic peak at 221°C corresponding to alginate-calcium interaction was observed. Similar results were reported by Fernandez-Hervas et al.[31] The papain exhibits a sharp endothermic peak at 196°C, whereas the melting peak shape of papain-loaded alginate beads was similar to the blank beads and did not show any peak at 196°C. This confirms that most of the enzyme was uniformly dispersed at the molecular level in the beads.
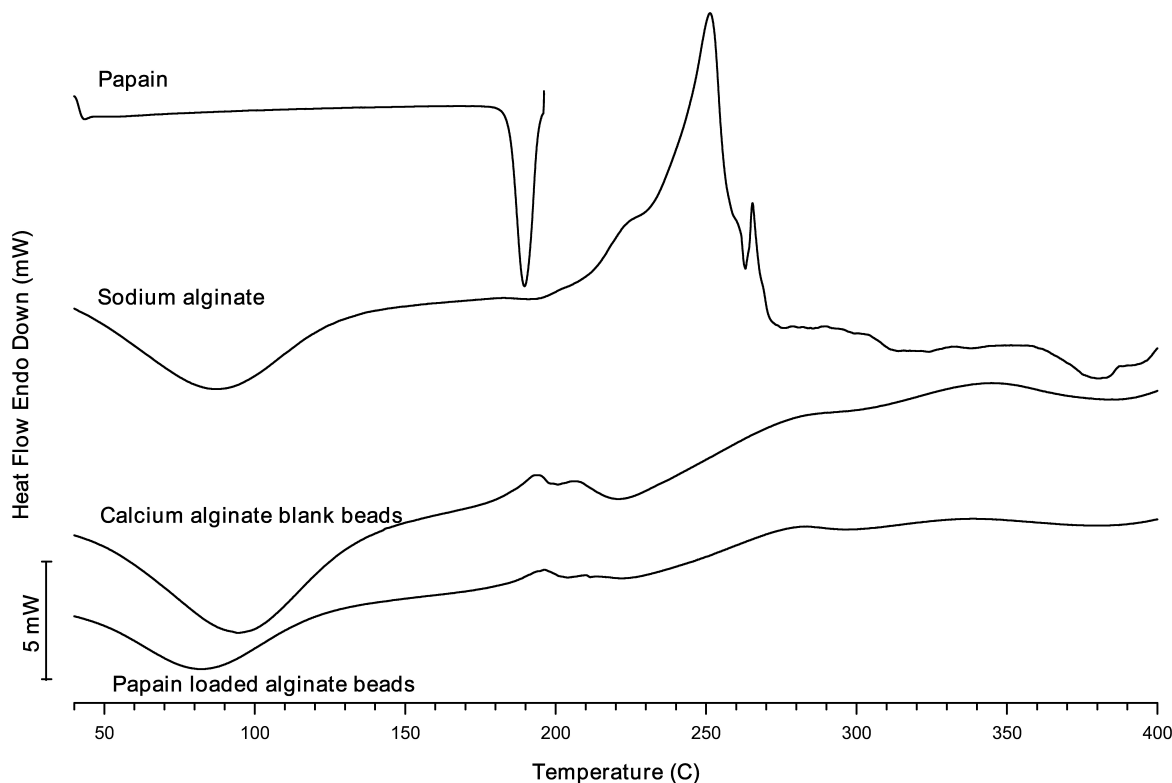
Figure 5. The DSC thermograms of papain, sodium alginate, blank calcium alginate beads, and papain-loaded alginate beads made at the same analytical conditions.

Morphology of the Beads

The spherical shape of beads in the wet state was usually lost after drying, especially for beads prepared with low alginate concentration. In 1% (w/v) alginate, the dried beads were very irregular and tended to agglomerate because of low mechanical strength. With the increasing of alginate concentration (2% w/v), the shape of beads changed to a spherical disk with a collapsed center (Figure 6). Normally the spherical shape was retained when the alginate concentration was as high as 5% (w/v), but viscosity of 5% w/v solution was too high for bead preparation under the present experimental conditions, so it was not studied. These results indicated that the shape of calcium alginate beads was seriously destroyed in the drying process, and the spherical shape of dried beads improved with the increase of alginate concentration. It was reported by Skjak-Brae et al[32] that calcium alginate beads usually have a heterogeneous structure with a dense surface layer and a loose core because of the heterogeneous gelation mechanism, which resulted in the collapse of beads during the drying process.

Stability Study

For the developed formulation, the similarity factor was calculated by a comparison of the dissolution profiles at each storage condition with the control at the initial condition. Results of similarity factors ranged from 76 to 98 or 2% to 5% average difference. In addition to the dissolution profiles, capsule potency results for all of the stability conditions were within 90% to 110% of the label claim. Overall, results from the stability studies indicated that capsules were physically and chemically stable for ≥ 12 months at $40 \pm 2°C/75 \pm 5$% relative humidity and for >12 months (approximately for double time period) at $30 \pm 2°C/65 \pm 5$% relative humidity.

An approach for analyzing the data on a quantitative attribute that is expected to change with time is to determine the time at which the 95% 1-sided confidence limit for the mean curve intersects the acceptance criterion (≤ 5% change in assay from its initial value). The accelerated stability data for prepared formulation, marketed formulation,
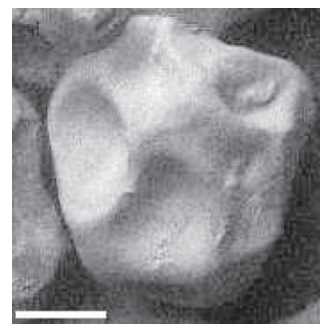

Figure 6. The scanning electron micrograph of dried alginate bead at $\times 100$ magnification (bar at the left bottom = 100 μm).
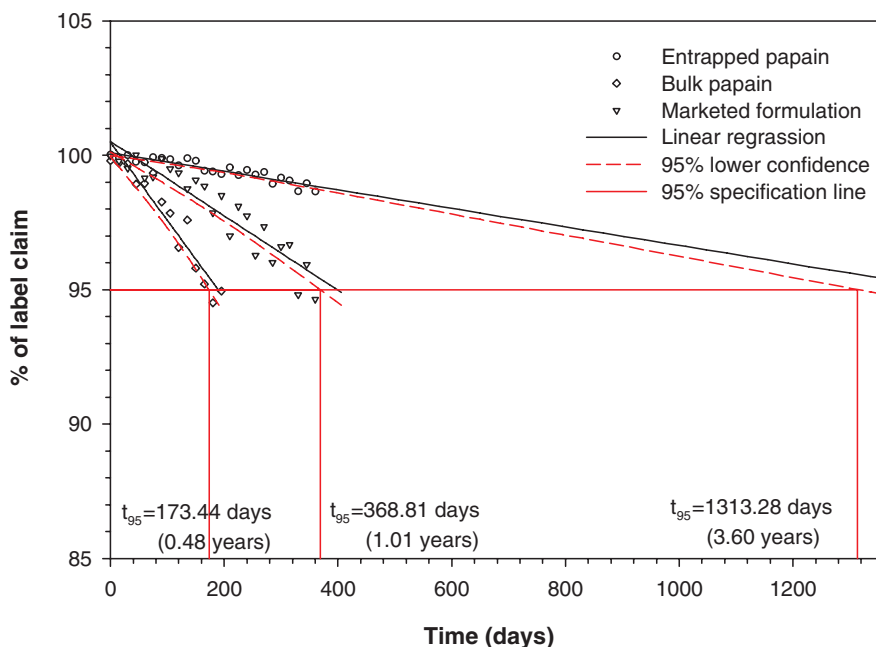
Figure 7. Extrapolation of accelerated stability data of developed formulation, marketed formulation, and bulk papain for shelf-life calculation.

and the bulk papain were extrapolated to calculate the shelf-life (Figure 7) and were found be 3.60 years, 1.01 years, and 0.48 years, respectively. Hence, the stability of the entrapped papain was significantly more improved than the conventional dosage forms.

CONCLUSIONS

The optimization of the process using the NN-predicted responses resulted in >90% entrapment and <10 minutes of T_{50} at low levels of all 3 of the process variables (1.0% sodium alginate, 0.05 mol/L calcium chloride, and 20 minutes hardening time). Entrapment of papain in alginate beads was confirmed using FTIR and DSC study. Texture analysis of the beads formulations illustrated that the degree of cross-linking decreased with an increase in sodium alginate concentration, whereas it increased with an increase in calcium chloride concentration and hardening time. Dissolution studies over a pH range similar to the human gastrointestinal tract demonstrated that alginate beads can be used for site-specific intestinal delivery of papain. An accelerated and long-term stability study illustrated considerable improvement in the shelf-life of papain entrapped in alginate beads than the conventional dosage form.

ACKNOWLEDGMENTS

REFERENCES

1. Bickerstaff GF. Immobilization of enzymes and cells: some practical considerations. In: Bickerstaff GF, ed. *Immobilization of Enzymes and Cells.* Totowa, NJ: Humana Press; 1997;1-12.

2. Uhlig H. *Industrial Enzymes and their Applications.* New York: Wiley; 1998.

3. Lin SY. Release kinetics of drug from different combined ratios of micropellets. *J Microencapsul.* 1993;10:319-322.

4. Ritschel WA. Targeting in the gastrointestinal tract: new approaches. *Methods Find Exp Clin Pharmacol.* 1991;13:313-336.

5. Chen H, Langer R. Magnetically-responsive polymerized liposomes as potential oral delivery vehicles. *Pharm Res.* 1997;14:537-540.

6. Park PG, Shalaby WSW, Park H. Physical Gels. In: *Biodegradable Hydrogels for Drug Delivery.* Lancaster, PA: CRC Press; 1993:99-140.

7. Yotsuyanagi T, Ohkubo T, Ohhashi T, Ikeda K. Calcium-induced gelation of alginic acid and pH-sensitive reswelling of dried gels. *Chem Pharm Bull.* 1987;35:1555-1563.

8. Pillay V, Dangor CM, Govender T, Moopanar KR, Hurbans N. Drug release modulation from crosslinked calcium alginate microdiscs. 1. Evaluation of the concentration dependency of sodium alginate on drug entrapment capacity, morphology and dissolution rate. *Drug Deliv.* 1998;5:25-34.

9. Arica B, Calis S, Kas HS, Sargon MF, Hincal AA. 5-Fluorouracil encapsulated alginate beads for the treatment of breast cancer. *Int J Pharmaceut.* 2002;242:267.

10. Gu F, Amsden B, Neufeld R. Sustained delivery of vascular endothelial growth factor with alginate beads. *J Control Release.* 2004;96:463.

11. Almeida FP, Almeida AJ. Cross-linked alginate-gelatine beads: a new matrix for controlled release of pindolol. *J Control Release.* 2004;97:431-439.

12. Agatonovic-Kustrin S, Zecevic M, Zivanovic LJ, Tucker IG. Application of artificial neural networks in HPLC method development. *J Pharm Biomed Anal.* 1998;17:69-76.

13. Sathe PM, Venitz J. Comparison of neural network and multiple linear regression as dissolution predictors. *Drug Dev Ind Pharm.* 2003;29:349-355.

14. Takayama K, Fujukawa M, Obata Y, Morishita M. Neural network based optimization of drug formulations. *Adv Drug Del Rev.* 2003;55:1217-1231.

15. Agatonovic-Kustrin S, Beresford R. Basic concepts of artificial neural network (ANN) modeling and its application in pharmaceutical research. *J Pharm Biomed Anal.* 2000;22:717-727.

16. Winkler DA, Burden FR. Bayesian neural nets for modeling in drug discovery. *Drug Discovery Today: BIOSILICO.* 2004;2:104-111.

17. Turner JV, Maddalena DJ, Cutler DJ. Pharmacokinetic parameter prediction from drug structure using artificial neural networks. *Int J Pharm.* 2004;270:209-219.

18. Veng-Pedersen P, Modi NB. Application of neural networks to pharmacodynamics. *J Pharm Sci.* 1993;82:918-926.

19. Kachrimanis K, Karamyan V, Malamataris S. Artificial neural networks (ANNs) and modeling of powder flow. *Int J Pharm.* 2003;250:13-23.

20. Havlis J, Madden JE, Revilla AL, Havel J. High-performance liquid chromatographic determination of deoxycytidine monophosphate and methyldeoxycytidine monophosphate for DNA demethylation monitoring: experimental design and artificial neural networks optimisation. *J Chromatogr B Biomed Sci Appl.* 2001;755:185-194.

21. Dow LK, Kalelkar S, Dow ER. Self-organizing maps for the analysis of NMR spectra. *Drug Discovery Today: BIOSILICO.* 2004;2:157-163.

22. Lim CP, Quek SS, Peh KK. Prediction of drug release profiles using an intelligent learning system: an experimental study in transdermal iontophoresis. *J Pharm Biomed Anal.* 2003;31:159-168.

23. Taskinen J, Yliruusi J. Prediction of physicochemical properties based on neural network modelling. *Adv Drug Deliv Rev.* 2003;55:1163-1183.

24. Molnar L, Keseru GM, Papp A, Gulyas Z, Darvas F. A neural network based prediction of octanol-water partition coefficients using atomic5 fragmental descriptors. *Bioorg Med Chem Lett.* 2004;14:851-853.

25. Jouyban A, Majidi M-R, Jalilzadeh H, Asadpour-Zeynali K. Modeling drug solubility in water-cosolvent mixtures using an artificial neural network. *Farmaco.* 2004;59:505-512.

26. Iannuccelli V, Coppi G, Bernabei MT, Cameroni R. Air compartment multiple-unit system for prolonged gastric residence. Part I. Formulation study. *Int J Pharm.* 1998;174:47-54.

27. Wang K, He Z. Alginate-konjac glucomannan-chitosan beads as controlled release matrix. *Int J Pharm.* 2002;244:117-126.

28. Kim C-K, Lee E-J. The controlled release of blum dextran from alginate beads. *Int J Pharm.* 1992;79:11-19.

29. Ostberg T, Lund EM, Graffner C. Calcium alginate matrices for oral multiple unit administration. IV Release characteristics in different media. *Int J Pharm.* 1994;112:241-248.

30. Wong TW, Chan LW, Kho SB, Heng PWS. Design of controlled-release solid dosage forms of alginate and chitosan using microwave. *J Control Release.* 2002;84:99-114.

31. Fernandez-Hervas MJ, Holgado MA, Fini A, Fell JT. In vitro evaluation of alginate beads of a diclofenac salt. *Int J Pharm.* 1998;163:23-34.

32. Skjak-Brae G, Grasdalen KH, Draget KI, Smidsrod O. Inhomogeneous poysaccharide ionic gels. *Carbohydr Polym.* 1989;10:31-54.